

UDC:551.465:551.5(262.3)
Conference paper

MODELLING OF TIDAL AND WIND-INDUCED CURRENTS AND DISPERSION IN THE NORTHERN ADRIATIC

MODELIRANJE STRUJANJA IZAZVANOG MORSKIM MIJENAMA I VJETROM I DISPERZIJE U SJEVERNOM JADRANU

R. Rajar and M. Četina

*University of Ljubljana, Faculty of architecture, civil enrg. and surveying,
Ljubljana, Slovenia*

A three-dimensional nonlinear baroclinic model, developed at the Departments for Civil Engineering, University of Ljubljana, is described first. In the model, the "vertical" turbulent viscosity is computed by a one-equation turbulence model of Koutitas, while constant "horizontal" turbulent viscosity is utilized.

Tidal circulation in the Gulf of Trieste is computed by the model. The M2 tidal constituent is used for boundary condition at the open boundary. To determine tidal circulation in the smaller Piran Bay and Koper Bay, the s.c. nested models are used, the results from the larger region being used as boundary conditions for smaller regions. Current measurements along the Slovenian coast, executed by members of the Water Management Institute in Ljubljana in 1984 to 1986, are used for verification. The agreement is relatively good. Both measurements and simulation show a cyclonic gyre in Koper Bay during falling tide and residual current of the order 3-6 cm/s was found in Koper Bay in the E to N direction. Measurements also show an indication of a weak residual E to NE current along the whole Slovenian coast towards Trieste, the order of magnitude being about 1 to 3 cm/s.

Dispersion of pollutant from Rižana River into the Koper Bay is simulated further and compared qualitatively with measurements of dispersion of faecal pollution in the bay.

Simulation of wind - induced circulation in the Northern Adriatic was performed with the same 3D model, where the transport and dispersion of the Po River water was also simulated. For Bura wind (NE) the simulated circulation shows a very good agreement with a satellite image, based on chlorophyll concentration (from Kuzmić). Bura and Sirocco (SE) winds are simulated under

winter (no stratification) and summer conditions (temperature and salinity stratification). Both for NE and SE winds the simulation shows that a part of the polluted Po River water is transported towards Slovenian and Croatian coast.

INTRODUCTION

The water quality along the Slovenian coast is mainly not satisfactory. Especially in Koper Bay some measurements of chemical and biological parameters have shown very bad water quality (Olivotti *et al.*, 1985).

Investigations began in 1984 with the final goal to develop a combined hydrodynamical-water quality mathematical model, which would be a very useful tool for designing and planning different measures for the improvement of water quality. When such a model is verified and calibrated, it is possible to simulate different existing and planned situations and measures and it can give answers to different questions such as:

- what are optimum locations of wastewater outfalls?
- what is the minimum necessary degree of purification before discharging the waste water into the sea?
- what will be the concentration of different parameters at some important locations (beaches, marinas, harbours)?
- what would be the extent of oil spreading in the case of an ecological catastrophe i.e., oil spill from tankers or from pipes?

First, measurements of physical parameters (currents, temperature, salinity, wind) must be made in order to have a solid basis for the verification of the hydrodynamical model. In addition, water quality parameters must be measured for the verification of the water quality model.

In our investigation, up to now, the current velocities in the Koper Bay and Piran Bay (which are the parts of the Gulf of Trieste) were measured and the hydrodynamical mathematical model was developed, verified, and also calibrated. This model can simulate current velocities, and the transport and dispersion of passive pollutants (without changing their overall mass with time due to bio-chemical reactions). The flow due only to tides i. e., without winds, was simulated first by the mathematical model in the whole Gulf of Trieste and then in its parts, Piran and Koper Bay. The transport and dispersion of pollutants from the Rižana River into Koper Bay was simulated and compared qualitatively with some measurements.

A satellite image of currents in the northern Adriatic after five days of Bura wind gave us a very good basis for the verification of the mathematical model. Computed velocity fields for Bura (NE) and Sirocco (SE) wind for winter and summer conditions are presented.

CURRENT MEASUREMENTS

Measurements of currents were made from 1984 to 1986 by a team of specialists from the Water Management Institute in Ljubljana, together with members of the Polish Academy of Science (Tonin, 1986). The measurements were made by velocity meters from a boat in Piran Bay at every meter of the depth, and in Koper Bay at three depths. The measurements were made two to six times in 24 hours at six locations in the Piran Bay (locations being shown in Fig. 7) in the wider area of the Gulf of Trieste (Fig. 1). One autonomous current meter was installed at the entrance of Piran Bay recording current velocities at two depths.

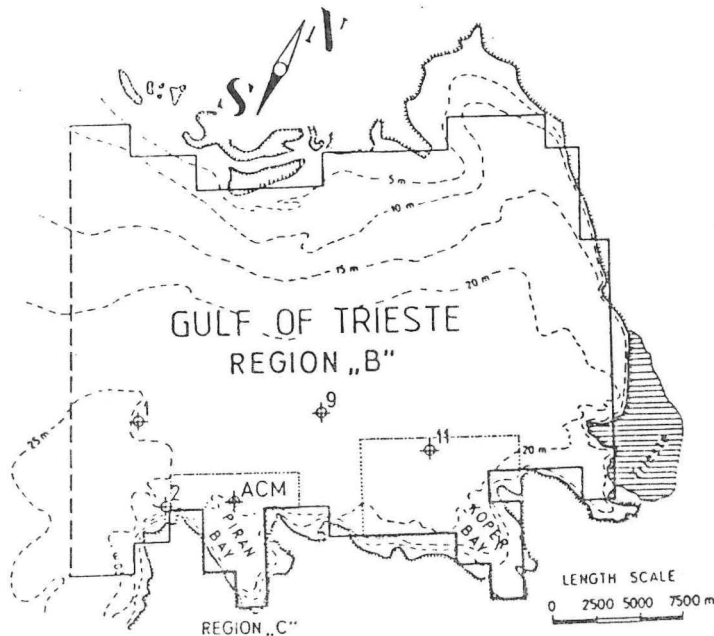


Fig. 1. Region B (Gulf of Trieste) with the locations of measurements

At the same time the following parameters were measured: temperature, salinity, local wind velocity and direction, and the hourly mean velocity at the coastal station Beli Križ in Piran. Fig. 2 shows the measured currents at pt. 4 in the Piran Bay. The measurements in Piran Bay were made during spring and summer months (May through July). Relatively strong stratification was recorded during most of the measurements. The measurements in Koper Bay were performed in autumn (end of September through

November). Almost no stratification was to be observed during that time.

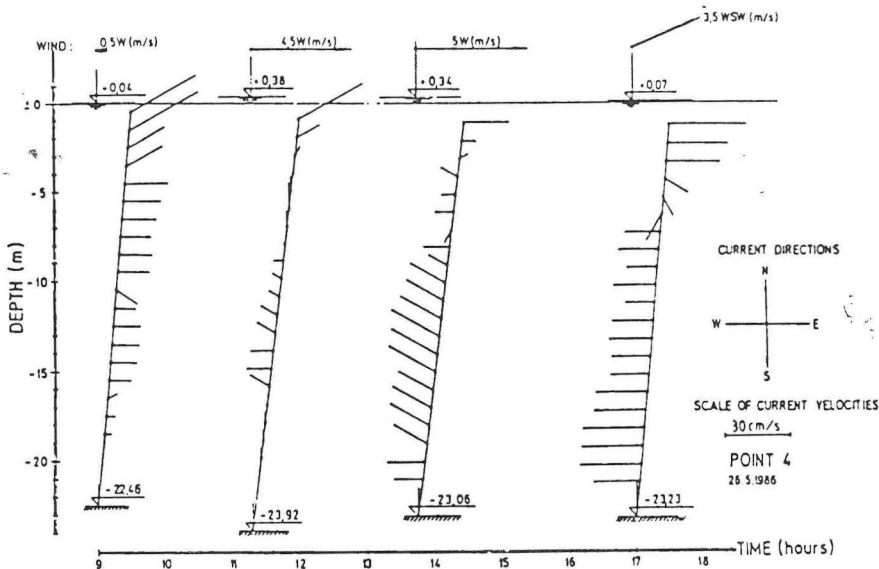


Fig. 2. Measured current velocities at Pt. 4 in Piran Bay

Since for all locations of measurements except the autonomous current meter, only separate instantaneous measurements were taken, the following values were calculated after the analysis of results. All the measurements were divided into three groups:

- wind less than 2 m/s (for surface currents) and less than 4 m/s (for bottom currents)
- Bura wind (NE)
- Sirocco wind (S, SE).

In this paper we are mostly concerned with the measurements of group (a) where the wind does not have a perceptible effect on the currents, they are only due to tidal forcing. This group of measurements were divided into the following subgroups:

- measurements during rising tide
- measurements during peak water level
- measurements during falling tide
- measurements during minimum water level
- average of all the measurements of group (a).

Average surface and average bottom velocities for the mentioned subgroups were calculated in addition to the depth average values.

MATHEMATICAL MODEL

Description

The mathematical model is 3-dimensional and based on the so-called "grid-box" method (Fig. 3) where the flow field is divided into control volumes (C.V.). The surface layer "breathes" with the water surface, while all the other layers are fixed in time. The meaning of the symbols in Fig. 3 and Eqs. 1 to 8 is: u, v, w - velocity components, h - thickness of C.V., H - depth, ζ - density, p - pressure, p_a - atmospheric pressure, T - temperature, s - salinity, N_u, N_v - coefficients, t - time, f - Coriolis parameter, τ_w - wind stress, τ_b - bottom stress (expressed by quadratic Manning's formula).

Basic equations

The following equations can be written:

$$\frac{\partial h}{\partial t} + \frac{\partial(hu)}{\partial x} + \frac{\partial(hv)}{\partial y} + w_u - w_d = 0 \quad (1)$$

$$\begin{aligned} \frac{\partial(hu)}{\partial t} + \frac{\partial(hu^2)}{\partial x} + \frac{\partial(huv)}{\partial y} + \frac{\partial(huw)}{\partial z} = +fvh - \frac{h}{\rho} \frac{\partial p}{\partial x} + \\ + \frac{\partial}{\partial x} [hN_h \frac{\partial u}{\partial x}] + \frac{\partial}{\partial y} [hN_h \frac{\partial u}{\partial y}] + \frac{\partial}{\partial z} [hN_v \frac{\partial u}{\partial z}] + \frac{1}{\rho} \tau_{wx} - \frac{1}{\rho} \tau_{bx} \end{aligned} \quad (2)$$

$$\begin{aligned} \frac{\partial(hv)}{\partial t} + \frac{\partial(huv)}{\partial x} + \frac{\partial(hv^2)}{\partial y} + \frac{\partial(hvw)}{\partial z} = -fuh - \frac{h}{\rho} \frac{\partial p}{\partial y} + \\ + \frac{\partial}{\partial x} [hN_h \frac{\partial v}{\partial x}] + \frac{\partial}{\partial y} [hN_h \frac{\partial v}{\partial y}] + \frac{\partial}{\partial z} [hN_v \frac{\partial v}{\partial z}] + \frac{1}{\rho} \tau_{wy} - \frac{1}{\rho} \tau_{by} \end{aligned} \quad (3)$$

$$\frac{\partial p}{\partial z} + \rho g = 0 \quad \rightarrow \quad p = p_a + g \int_z^H \rho dz \quad (4)$$

$$W_K = - \int_z^H \left(\frac{\partial(uh)}{\partial x} + \frac{\partial(vh)}{\partial y} \right) dz \quad (5)$$

$$\frac{\partial(hT)}{\partial t} + \frac{\partial(huT)}{\partial x} + \frac{\partial(hvT)}{\partial y} + \frac{\partial(hwT)}{\partial z} = \frac{\partial}{\partial x} \left[hD_h \frac{\partial T}{\partial x} \right] + \frac{\partial}{\partial y} \left[hD_h \frac{\partial T}{\partial y} \right] + \frac{\partial}{\partial z} \left[hD_v \frac{\partial T}{\partial z} \right] \quad (6)$$

$$\frac{\partial(hs)}{\partial t} + \frac{\partial(hus)}{\partial x} + \frac{\partial(hvs)}{\partial y} + \frac{\partial(hws)}{\partial z} = \frac{\partial}{\partial x} \left[hD_h \frac{\partial s}{\partial x} \right] + \frac{\partial}{\partial y} \left[hD_h \frac{\partial s}{\partial y} \right] + \frac{\partial}{\partial z} \left[hD_v \frac{\partial s}{\partial z} \right] \quad (7)$$

$$\rho = \rho(T, s) \quad (8)$$

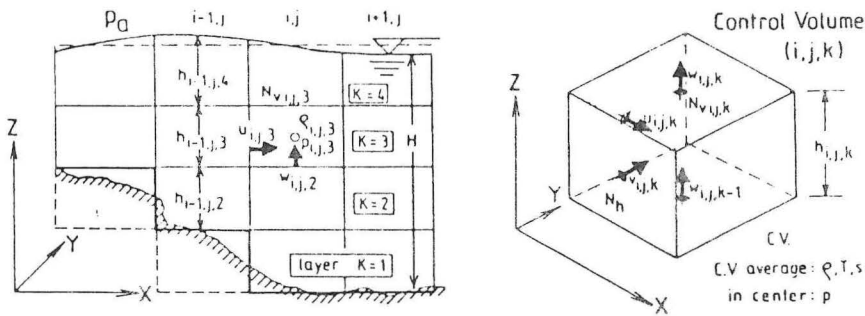


Fig. 3. Scheme of the 3D mathematical model

From eight equations we must determine eight unknown parameters: u, v, w, h, p, ζ, s and T . An important feature of the model is that it can simulate the transport and

dispersion of salinity or heat or in the same form any "passive" pollutant. These parameters influence the density by the equation of state (Eq. 8). Density changes then influence the velocity field at the next time step.

To obtain the "water quality model", we must add one equation in the form of Eq. 6 or 7 for every biological or chemical parameter (e.g. oxygen, phosphorus, BOD, algae etc.) to compute their transport and dispersion. The so-called "source terms" must be added on the right side of the equation to take into account the degradation of matter due to bio-chemical reactions.

Turbulence models

As we can see from Eqs. 2 and 3, we have used the well known Boussinesq approximation for the Reynolds stress between the C.Vs. Different "turbulent viscosities" are used for the stresses in the xz and yz plains (N_{Hl}) and in the xy plain (N_v). We use the known k - ϵ turbulence model for solving 2D problems but for several reasons we use more simple turbulence models in 3D modelling. First, some parameters of the k- ϵ model are badly defined. Second, the programming in 3D becomes complex and time consuming and third, our experiences have shown (Rajar *et al.*, 1986) that when computing the currents in large water bodies a constant values of N_{Hl} can give good results if the order of magnitude of N_{Hl} is well estimated. We have seen that the results are much more sensitive to the choice and distribution of N_v (Rajar *et al.*, 1989b). Therefore, for the computation of N_v we use a simplified one-equation turbulence model of Koutitas (1980), which assumes a kind of parabolic distribution of N_v with depth, with a maximum value at 0.6 H and zero at the bottom and at the surface. The maximum value depends on the depth and on the surface wind stress.

Stable density stratification can strongly diminish the value of N_v . We use the Munk-Anderson experimentally obtained relation with N_v and D_v being dependent on the Richardson number (Rodi, 1980):

$$R_i = -\frac{g}{\rho} \frac{\frac{\partial \rho}{\partial z}}{\left[\frac{\partial u}{\partial z}\right]^2} \quad (9)$$

$$N_v = N_{v0} [1 + 10R_i]^{-0.5} \quad D_v = D_{v0} [1 + 3.33R_i]^{-1.5} \quad (10)$$

The values of turbulent viscosities and dispersion coefficients become more important

when we want to compute precisely the transport and dispersion of pollutants. We are preparing computations on the basis of s.c. Particle-Tracking Method, which is more accurate for the simulation of dispersion of pollutants.

In our 2D (depth averaged) mathematical model the K- ϵ turbulence model is included. This model calculates values of N_H at every space and time step. Since tidal flow is more or less 2D, we have made a computation with this model for tidal flow in the Koper Bay. The results were very similar to the computations with constant N_H (Fig. 8) so they are not discussed further.

Boundary conditions

The following boundary conditions can be taken into account:

- a. solid boundaries (with zero normal velocities)
- b. wind stress at the surface
- c. inflow of rivers
- d. changing atmospheric pressure
- e. known tidal function at the open boundary
- f. the "radiation condition" at the open boundary
- g. the "continuity" boundary condition at the open boundary
- h. known distribution of velocities at the open boundaries (e. g. obtained from computations of larger flow field)
- i. given heat flux at the surface
- j. known temperature and salinity conditions at the boundaries (e.g. at the river inflow).

We have introduced the so called "continuity boundary condition" after the idea of Stravisi (1977). The assumption that the inflow equals the outflow is accounted for at the open boundary by using vertically averaged velocities in the boundary cross-section. Otherwise, the wind stress causes inordinately high velocities at the surface.

For computing tidal flow in Piran Bay and Koper Bay, boundary conditions a, e and h were used, while for computing the wind induced flow in the Northern Adriatic, boundary conditions a, b, c, f, g and j were taken into account.

TIDAL CURRENTS IN THE GULF OF TRIESTE

The final goal of this part of the investigation was the determination of currents and dispersion in Piran Bay and in Koper Bay. However, to determine the boundary conditions at the open boundary of the two bays, we had to simulate first the whole Gulf of Trieste.

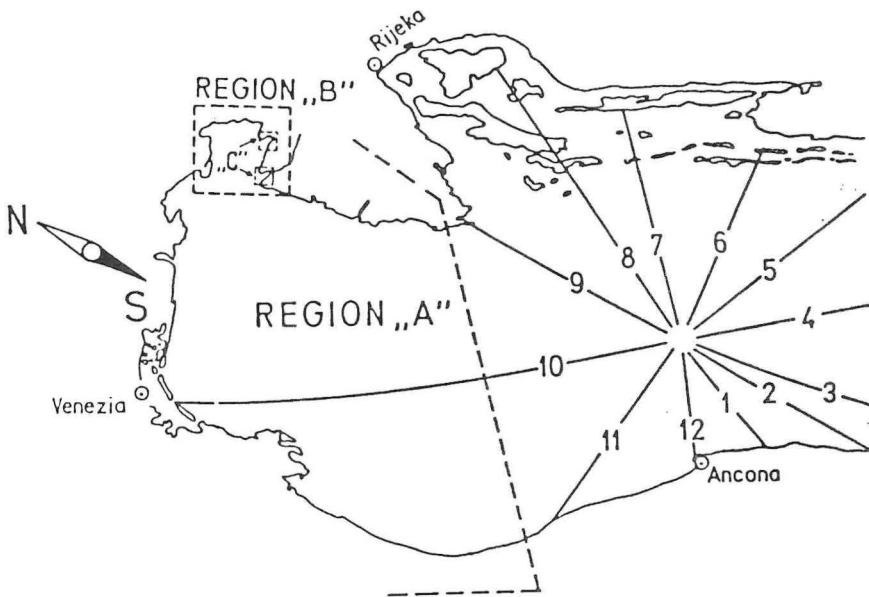


Fig. 4. Northern Adriatic with cotidal lines
Data for the computation

The following data were used in the analyses:
Dimensions of the flow field: 30600 x 27000 m
Numerical grid 19x17x5 (Figs. 5 and 6)
Space steps: $D_x = D_y = 1800$ m, $D_z = 4$ to 5 m
Time step: $D_t = 200$ sec
Turbulent viscosities: $N_h = 1.0$ m²/s, $N_v = 0.01$ m²/s (constant).

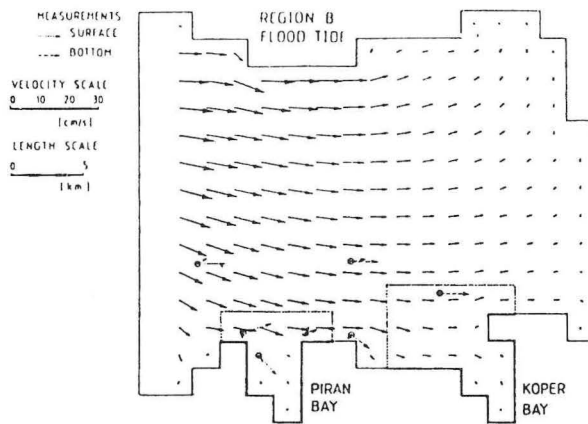


Fig. 5. Tidal currents in the Gulf of Trieste during rising tide

Because of the lack of exact data, a cotidal line was assumed at the entrance of the Gulf of Trieste. Fig. 4 shows that this assumption is not very far from reality. The M2 curve was taken into account at the open boundary, with the amplitude for Piran $a = 30$ cm. No phase lag was accounted for between N and S. More recently *M o s s e t t i* and *P u r g a* (1990) published that a phase lag existed between N and S.

Results

Figs. 5 and 6 show the tidal flow during rising and during falling tide (at the time of mean water level). During the rising tide the flow is mainly into the region, slightly deviated to the right due to the Coriolis effect, and deformed by the topographic effects in the interior of the Gulf. During falling tide the flow is mainly out of the region. Only currents in the surface region are presented, since in this case the flow is nearly two

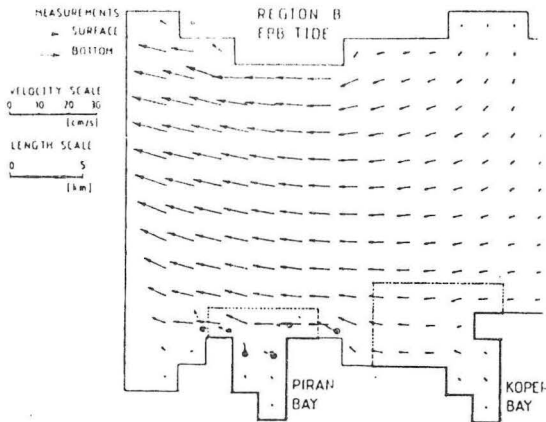


Fig. 6. Tidal currents in the Gulf of Trieste during falling tide

dimensional. Because of bottom friction, only velocities in the bottom layer are lower.

Maximum computed velocities are on the whole up to 10 cm/s, locally up to 12 cm/s. Comparison with the current field computed by the 2D mathematical model of Lang et al., (1990) shows that they obtained slightly lower velocities (up to 9 cm/s), which is probably due to the fact that they used an amplitude of the M2 curve of 25 cm. But the overall pattern of the flow field is comparable to the ones in Figs. 5 and 6.

TIDAL CURRENTS IN PIRAN BAY

Fig. 5 shows the boundaries of the computational field for Piran Bay and Koper Bay as "nested models". The velocities at these boundaries obtained from the large model (Gulf of Trieste) were used as boundary conditions for the computations of two smaller regions. Here a simplification was made: the computation inside the smaller computational regions was taken as quasi-steady with time of maximum velocities.

Data for computation

The following data were used in the computations:
Dimensions of the flow field: 7650 x 7650 m
Numerical grid: 19 x 19 x 5 control volumes
Space steps: $D_x = D_y = 450$ m $D_z = 4$ to 5 m
Time step $Dt = 300$ sec

Turbulent viscosities: $N_h = 0.2 \text{ m}^2/\text{sec}$, $N_v = 0.005 \text{ m}^2/\text{sec}$ (constant).

Results

The results are shown in Fig. 7a for the rising tide and in Fig. 7b for the falling tide together with the results of measurements i.e. average measured velocities in the surface

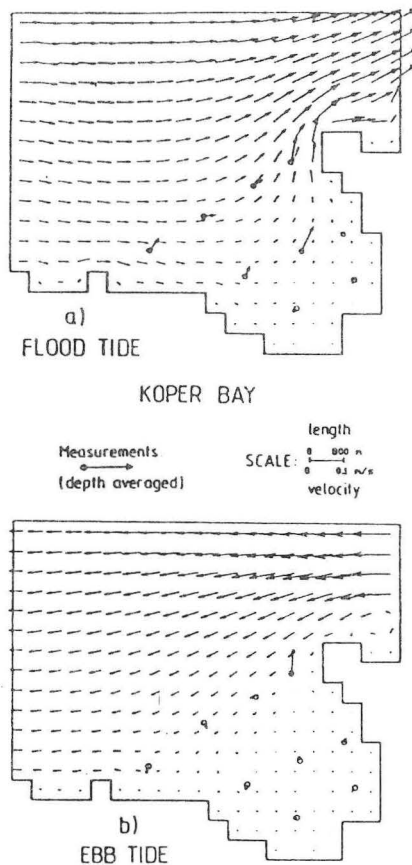


Fig. 7. Tidal currents in the Piran Bay a) during rising tide; b) during falling tide

layer and in the bottom layer. The agreement can be considered as satisfactory. Both computations and measurements show a flow along the coast that is mainly eastward during rising tide and westward during falling tide. The velocities are of the order of

10 cm/s at the entrance of the bay and smaller inside the bay. The currents are relatively convenient for the transport and dispersion of pollutants. The outlet from the Piran waste water treatment plant is relatively well located (Fig. 7a), though more to the west, velocities are a little greater.

TIDAL CURRENTS IN KOPER BAY

We assumed the same type of boundary condition for Koper Bay as Piran Bay.

Data for computation

The following data were used in the computations:

Dimensions of the flow field: 7650 x 9000 m

Numerical grid: 19 x 22 x 5 control volumes

Space steps: $D_x = D_y = 450$ m, $D_z = 4$ to 5 m

Time step: $D_t = 300$ sec

Turbulent viscosities: $N_h = 0.2$ m²/sec, $N_v = 0.005$ m²/sec (constant).

Results

The results are shown in Fig. 8a (rising tide) and Fig. 8b (falling tide) together with the measured vertically averaged velocities. The flow is towards the east and north along the coast during rising tide, but both computations and measurements show a cyclonic gyre during falling tide. The agreement with the measurements is good.

An indication for a residual current towards the east and north was found during the investigation and is discussed in the next section.

RESIDUAL CURRENTS IN THE GULF OF TRIESTE

To make a detailed analysis of the residual currents along the Slovenian coast, we do not have enough measured data. To make such an analysis with the mathematical model is very difficult. The model is able to simulate all the influences due to thermohaline forcing, is able to simulate all the influences due to thermohaline forcing, but we do not have enough data about the initial and boundary conditions. We should put into model the exact 3D distribution of temperature and salinity over the entire computational region (initial condition) and especially at the open boundaries where the velocity distribution should be known (boundary condition). In addition, the energy budget of the region (insolation, radiation, evaporation) should be accounted for. However, this is not yet

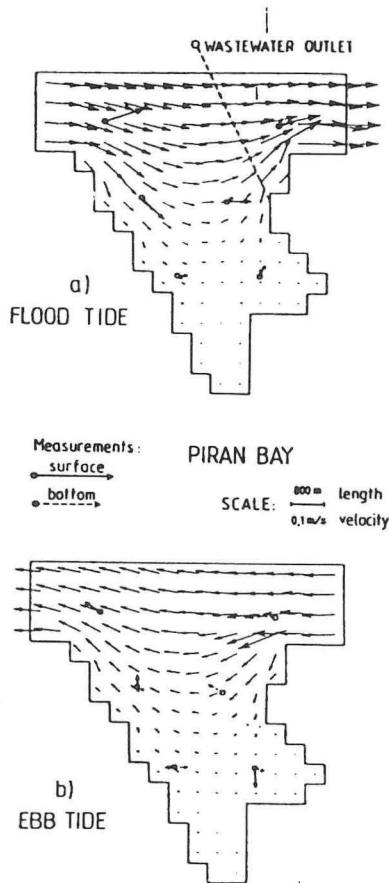


Fig. 8. Tidal currents in the Koper Bay a) during rising tide; b) during falling tide

contained in the present mathematical model. We plan to improve the model and to simulate the residual currents in the whole northern Adriatic in the next step of the research.

In spite of these limitations, we can make some preliminary estimations of the residual current along the Slovenian coast, i.e. the southern coast of the Gulf of Trieste.

The measured velocities in Figs. 7 and 8 show that the eastward currents during the rising tide are slightly stronger than the westward currents during the falling tide, and there is an indication of a weak residual current along the Slovenian coast towards E to NE, with velocities of the order 1 to 3 cm/s.

For the Koper Bay we have traced the average velocity vectors obtained by all the measurements (on windless day) in Fig. 9. It can be seen that at all the measured points

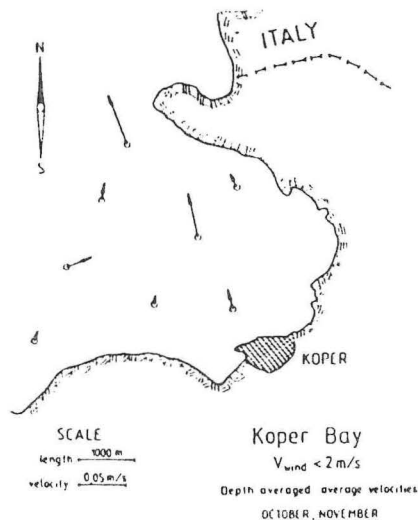


Fig. 9. Depth averaged average velocities in the Koper Bay

the average flow is along the coast in Koper Bay mainly in the northern direction. The order of magnitude of the residual current is about 3 cm/sec, while at two points the velocities reached 5 cm/s. In the interior of the bay current velocities are about 1 to 2 cm/s. One of the causes for this residual current is mentioned tidal circulation, since the cyclonic gyre at ebb tide causes the same flow direction as flood tide. The analysis of wind-induced circulation in Trieste Gulf and along the Slovenian coast (for Bura wind - ENE, Scirocco wind - SE and Maestral - WNW, R a j a r, 1992) confirms strongly the existence of mentioned residual circulation.

Fig. 10 shows a schematic presentation of surface circulation in the northern Adriatic as proposed by O r l i ć (1989). We have added to the figures the results of measurements from M o s s e t t i and P u r g a (1990) for the Gulf of Trieste and also our above mentioned results. Only the directions of the currents are presented.

The results of three sources are mainly in agreement. They show an eastern to northeastern current along the Slovenian coast.

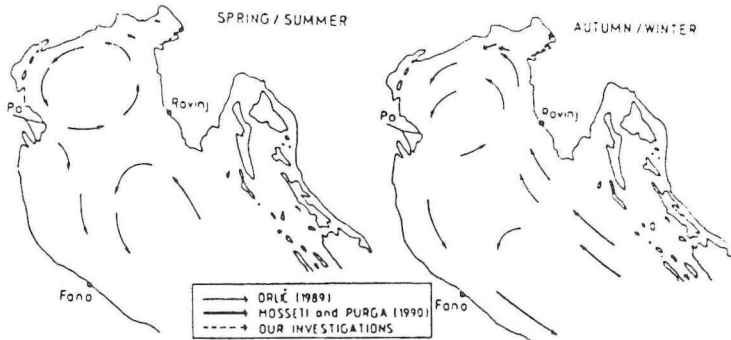


Fig. 10. Schematic representation of the surface currents in the Northern Adriatic (adapted from Orlić, 1989) Only directions of currents are presented

DISPERSION IN KOPER BAY

To verify our mathematical model we have also made a simulation of the transport and dispersion of pollutants from the Rižana River into Koper Bay.

The waste water treatment plant for the city of Koper (up to now only mechanical treatment) has its outlet into the Rižana River which discharges into the eastern part of the Koper Bay. Since we did not have exact data about the distribution of salinity and temperature in the bay or in the river, we simulated only the spreading of a hypothetical passive pollutant which does not influence the density of the water. In this case no stratification was taken into account.

At the open boundaries the velocity distribution obtained from the computation in the Gulf of Trieste was taken into account. To simulate realistically the transport and dispersion of the pollutant, unsteady conditions with tidal cycle M2 (with the period of 12.4 hours) were taken into account at the open boundaries. Besides, a residual eastern to northern current with the magnitude of 2 c/s was superimposed. This current increases the velocities during the rising tide and diminishes them during the falling tide.

The other data were the same as for the computation of the tidal currents in Koper Bay. Since the velocities near the mouth of the Rižana River are very small during the whole tide cycle (of the order 1 cm/s or less) we have simulated 45 hours of real time. Fig. 11 shows the computed isolines of the pollutant 45 hours after the beginning of the simulation together with a result of measurements of concentration of faecal pollution in summer 1980 - 1982 (Turk *et al.*, 1982). Only a qualitative comparison can be

Modelling of currents and dispersion in the Adriatic Sea

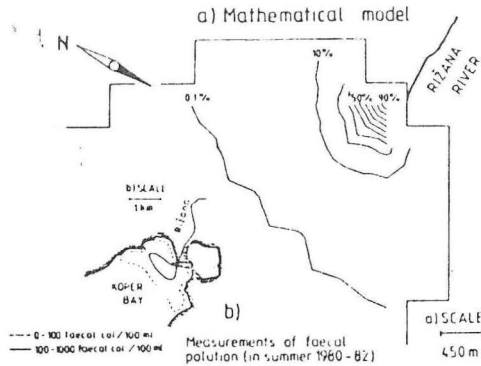


Fig. 11. a) Simulation of dispersion of pollutants from Rižana River
b) Measurements of faecal pollution (from Turk *et al.*)

made between the measured and computed distributions because no time development of the spreading was measured. However, qualitatively the form of the polluted region is comparable. Both computed and measured distributions are asymmetric (the center is north of the Rižana River mouth) which confirms the assumption of the residual eastern and northern current along the coast.

CIRCULATION DUE TO BURA WIND (NE) IN THE NORTHERN ADRIATIC

Introduction

By different estimates the Italian river Po contributes between 65 and 90% of all the pollutants brought into the Northern Adriatic. Therefore the simulation of the hydrodynamical circulation in this part of the Adriatic is very important. Especially the simulation of transport and dispersion of pollutants is of great interest i.e. under what weather conditions and in what concentrations the pollutants reach the Slovenian and Croatian coastal waters.

Quite a number of models deal with wind-induced circulation in the northern Adriatic, particularly with the circulation due to the most frequent winter wind, the Bura (NE). Stravisi (1977) made simulations using a two-dimensional (2D) mathematical model while Kuzmić and Orlić (1987) used a 3D linearized model. Kuzmić (1991) presented some very good satellite images of Bura-induced circulation in this part of the Adriatic and comparison with the computed velocity field was very good.

Since our mathematical model is 3D nonlinear and is also able to simulate the transport

and dispersion of passive pollutants, we made simulations of circulation due to the Bura (NE) and Scirocco (SE) winds, with the emphasis on the computation of dispersion of pollutants from the Po River. Since the surface current velocities due to wind forcing are up to 50 cm/s, while velocities due to tidal forcing are of the order of 10 to 20 cm/s, only wind forcing is taken into account in this study. However, thermohaline forcing (due to fresh water from the Po River) is accounted for although it has much smaller influence in this case.

Winter conditions

From Kuzmić (1991) we obtained a good satellite image (Fig. 13) based on chlorophyll concentrations for March 26, 1982. This image was taken at the end of a

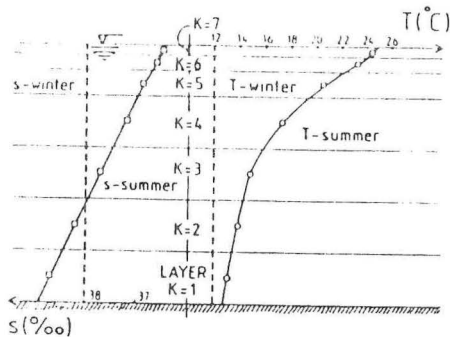


Fig. 12. Temperature and salinity distribution over depth - summer and winter conditions

five day period of Bura wind and presented a perfect opportunity for the verification of our mathematical model.

We used a $30 \times 29 \times 7$ numerical grid (Figs. 14 to 24). The space step was $\Delta x = \Delta y = 7500$ m and in the vertical direction the layers were situated at 2, 5, 10, 20, 30, 40 and 50 m (see Fig. 12). First, we simulated the winter conditions with temperature and salinity constant over the depth ($T = 12^\circ\text{C}$ and $S = 38\text{‰}$, Fig. 12). The Po River was simulated with $Q = 1500$ m³/s (Orlić, 1989), $T = 15^\circ\text{C}$ and $S = 18\text{‰}$. The turbulent viscosities were taken as $N_{II} = 100$ m²/s (constant) and the N_V distribution from Koutitas (1980) with $\Gamma = 1$. The radiation boundary condition was used.

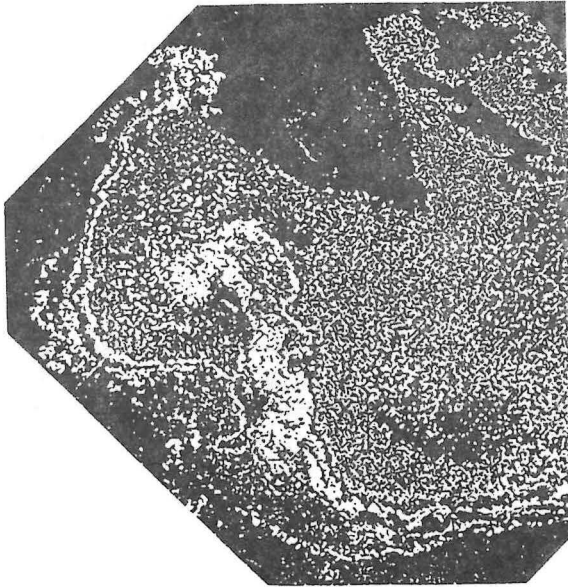


Fig. 13. Satellite image based on chlorophyll for March 26, 1982 (after five days of Bura wind) (from Kuzmić, 1991)

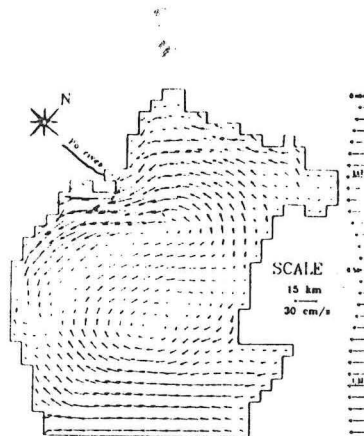


Fig. 14. Circulation in the surface layer, Bura wind, winter conditions

An important feature of the simulation is the nonuniform distribution of the wind proposed by Kuzmić and Orlić (1987). It is based on observations which show that the Bura wind is stronger in the Gulf of Trieste and in Kvarner Bay than

along the Istrian peninsula. Table 1 gives the coefficients of the wind distribution along the X axis (from SE to NW). The basic wind velocity was 7 m/s. The wind distribution is also presented in Fig. 14.

The comparison of Figs. 13 and 14 shows a very good agreement concerning the velocity field. Both the satellite image and the simulation show a cyclonic vortex and good agreement exists between the observed and computed vortex centers. Moreover, an anticyclonic vortex can be seen south of the first one. In addition, the spreading of

Table 1. Simulated heterogeneity in the wind field over the Northern Adriatic (adapted from K u z m i ć *et al.*, 1987) See also Fig. 14

i	factor	i	factor	i	factor	i	factor
2	1.18	10	1.19	18	0.69	26	1.34
3	1.23	11	1.00	19	0.88	27	1.23
4	1.27	12	0.85	20	1.15	28	1.08
5	1.30	13	0.73	21	1.35	29	0.90
6	1.32	14	0.65	22	1.43	30	0.69
7	1.32	15	0.58	23	1.47	31	0.42
8	1.30	16	0.56	24	1.47		
9	1.25	17	0.61	25	1.42		

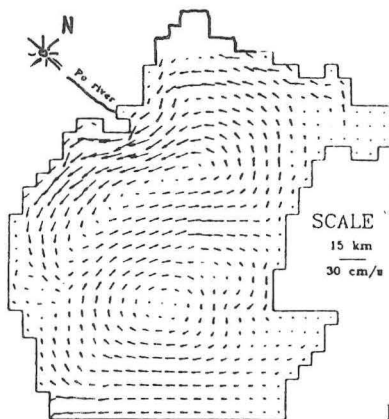


Fig. 15. Depth-averaged velocity pattern, Bura wind, winter conditions

salinity (Fig. 16) is mainly in agreement with the observed chlorophyll plume. The computed transport after five days of simulation did not reach so far as the observed ones, no doubt because of the assumption that the Po River outflow begins at time $t=0$ in the computation, while in reality the plume was already spread out before the period

of the Bura wind.

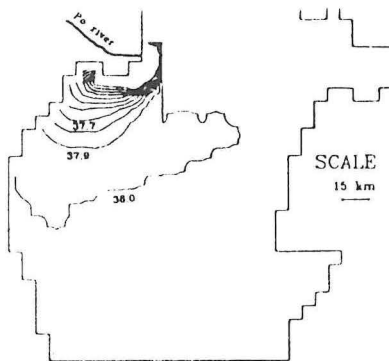


Fig. 16. Salinity distribution, Bura wind, winter conditions

The depth averaged velocity field (Fig. 15) is fairly similar to the circulation in the surface layer. This shows that at least under winter conditions the velocity distribution over the depth is approximately uniform and the flow is not far from being two-dimensional.

With good agreement with the observations confirms good applicability of the described model and also of the Koutitas distribution of the "vertical" turbulent viscosity N_v (see also R a j a r, 1989a).

Summer conditions

The summer conditions are characterized by the stratification in both temperature and salinity (see Fig. 12). Po River outflow is assumed to be $1200 \text{ m}^3/\text{s}$, with $T = 25^\circ\text{C}$ and $S = 18\text{‰}$. The depth averaged velocities under summer conditions are fairly close to the depth averaged circulation in the winter conditions (Fig. 15) so they are not presented here. The comparison of the velocity field in the surface layer (Fig. 17) with the depth averaged velocity field (Fig. 15) shows fairly different patterns. A number of computations have shown that this difference is due to a strong diminution of the vertical turbulent viscosity N_v , caused by the stable stratification according the Munk-Anderson relation (Eq. 10). No observations were available for summer conditions.

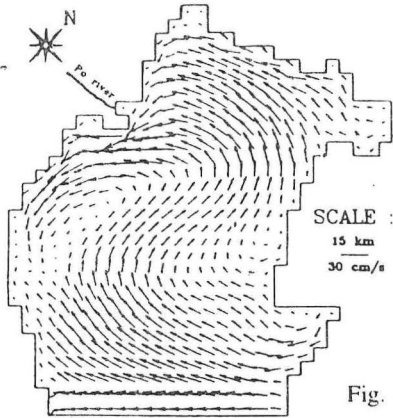


Fig. 17. Circulation in the surface layer, Bura wind, summer conditions

CIRCULATION DUE TO SIROCCO WIND (SE) IN THE NORTHERN ADRIATIC

Winter conditions

Fig. 18 shows the circulation in the surface layer due to the Sirocco wind (SE) of 10 m/s velocity. Fig. 19 shows the depth averaged velocities, while Fig. 20 shows the salinity distribution. The same assumptions for the computations were used for the Bura wind case (numerical grid, temperature and salinity distribution). Described "continuity" boundary condition was used at the open boundary.

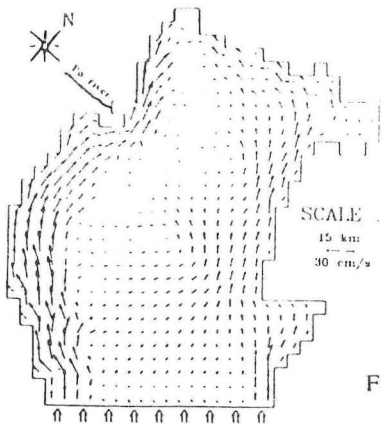


Fig. 18. Circulation in the surface layer, Sirocco wind, winter conditions

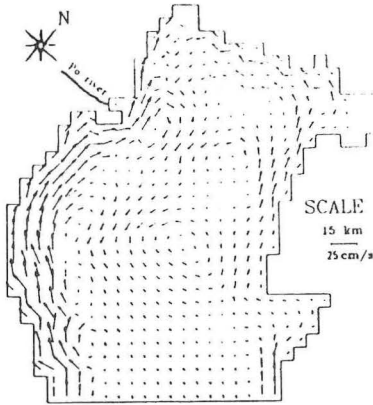


Fig. 19. Depth-averaged velocity pattern, sirocco wind, winter conditions

No comparison with the observations was possible, but the depth averaged velocities (Fig. 19) are in good agreement with Orlić (1988) where he simulated the whole Adriatic. This confirms the good applicability of the continuity boundary condition at least as far as the simulation of the velocity field is concerned.

A homogeneous wind field was assumed because of the lack of data on wind distribution. Orlić (1988) studied the effect of different wind distributions over the whole Adriatic but it seems that for the northern Adriatic the assumption of a uniform wind field is acceptable.

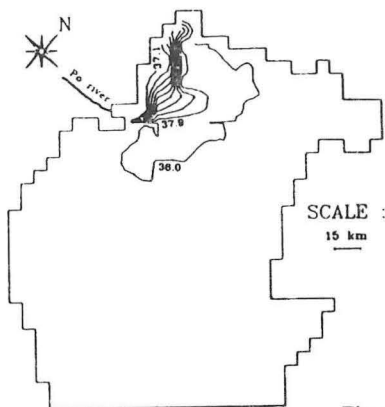


Fig. 20. Salinity distribution, Sirocco wind, winter conditions

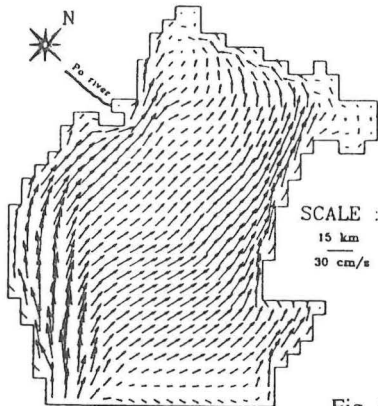
Summer conditions

Fig. 21. Circulation in the surface layer, Sirocco wind, summer conditions

Fig. 21 shows the velocity field in the surface layer due to the Sirocco wind (SE) in summer conditions. Fig. 22 shows the depth averaged velocities. As for Bura wind, under summer conditions the velocity distribution over the depth is more non-uniform than under winter conditions. Again, this is due to the effect of strong stable stratification on the distribution of turbulent viscosity N_V .

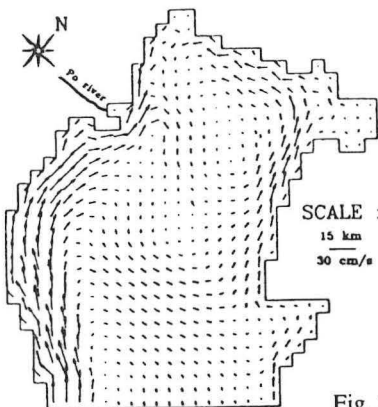


Fig. 22 Depth-averaged velocity pattern, Sirocco wind, summer conditions

We have seen that the "continuity" boundary condition, which we have introduced, has similar properties as the radiation boundary condition. The velocity field is properly

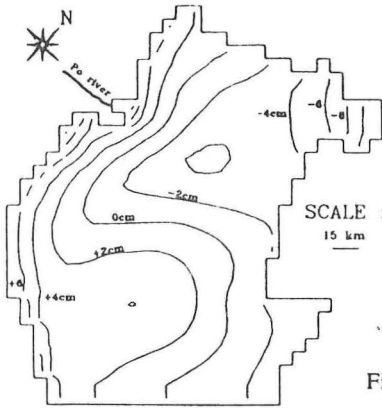


Fig. 23. Surface elevations, Bura wind, winter conditions

simulated. However, it is logical that in case when the wind direction is orthogonal to the open boundary, (Sirocco wind) super elevations of the water level, which would be caused in the (non simulated) southern and middle Adriatic, cannot be simulated in the partial model. But the relative elevations (and the gradient of the elevations) are simulated very well. The results are not very reliable only in the close vicinity of the open boundary. For example, in Fig. 18 it can be seen that close to the open boundary the surface velocities are not correct due to the fact that in the computation at the open boundary they are forced to be depth averaged.

Fig. 23 shows the surface elevations for the Bura wind, and Fig. 24 for the sirocco wind, both under winter conditions. The radiation boundary condition was used in the first case and the continuity boundary condition in the second case.

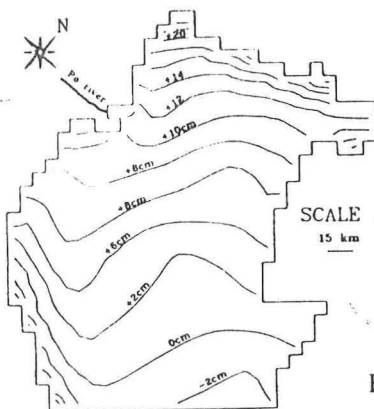


Fig. 24. Surface elevations, Sirocco wind, winter conditions

CONCLUSIONS

1. The described 3D baroclinic model was verified with different cases of measurements. It can be used as an efficient tool for the simulation of different existing or planned situations of hydrodynamical circulation and of transport and dispersion of pollutants. Optimum solutions in economic and environmental sense can be determined using the described model.
2. In the Gulf of Trieste a simulation of tidal forcing without wind was performed. During the rising tide the flow is roughly into the Gulf with maximum velocities being around 10 cm/s. During the falling tide the flow is mainly out of the gulf with deviations due to the effects of Coriolis acceleration and to topography.
3. Simulations of tidal currents in the smaller Piran Bay and Koper Bay were made as "nested models" and used the boundary conditions from the computations of larger region B (Gulf of Trieste). In Piran Bay both the simulation and the measurements show the flow along the coast and mainly eastward during the rising tide. During the falling tide, the flow is in the opposite direction. In Koper Bay the pattern is similar during rising tide, but a cyclonic gyre is formed in the bay during falling tide.
4. An indication was found that a weak residual current is present along the Slovenian coast toward the east and northeast at least under summer conditions. Current velocities are of the order of 2-3 cm/s. This is mainly in agreement with observations of Orlić (1989) and Mossetti and Purga (1990) - (Fig. 10) and also with some more recent analysis of currents along Slovenian Coast (Rajar, 1992).
5. Simulation of transport and dispersion of pollutants from the Rižana River into Koper Bay was compared with the measurements of faecal pollution. Agreement is qualitatively good. Again an asymmetric distribution of the pollutant confirms the assumption of the east to northeast residual current.
6. The comparison of the satellite image of the Northern Adriatic for the situation after five days of Bura wind with the simulated velocity field and salinity distribution shows very good agreement, which confirms the good applicability of described mathematical model. The forcing due to the scirocco wind (SE) was also simulated both under winter and summer conditions.
7. Under winter conditions (no stratification) the velocity distribution over the depth is fairly uniform. Under summer conditions it is much less uniform due to the diminution of the turbulent viscosity N_v and the reduction of shear stress between the layers, due to the stable stratification.
8. The results of the simulation show that both Bura and Sirocco wind cause the transport and dispersion of the pollutants from the Po River towards the center of the Northern Adriatic and also partly towards Slovenian and Croatian waters.
9. The effect of tidal and thermohaline forcing (without wind) on the transport and dispersion of pollutants from the Po River under winter and summer conditions will be studied next.

REFERENCES

- K o u t i t a s, C. 1980. Modelling three-dimensional wind induced flows. Proceedings ASCE, HY 11: 1843-1865.
- K u z m i ć, M. and M. O r l i ć. 1987. Wind induced vertical shearing ALPEX/MEDALPEX data and modelling exercise. *Annales Geophysicae*, 1: 103-112.
- K u z m i ć, M. 1991. Exploring the effect of Bura over the Northern Adriatic - CZS imagery and a mathematical model prediction. *Internat. J. Rem. Sensing*, 1.
- L a n g o, R., F. R a i c i c h and R. M o s s e t t i. 1990. A numerical model of transport and diffusion of radionuclides in the Gulf of Trieste. *Boll. Oceanogr. Teor. Appl.*, 1 : 13-24.
- M o s s e t t i, F. and N. P u r g a. 1990. Courants cotiers de différente origine dans un petit golfe (Golfe de Trieste). *Boll. Oceanogr. Teor. Appl.*, 1 : 51-62.
- O l i v o t t i, R., J. F a g a n e l i and A. M a l e j. 1985. Eutrophication of coastal waters - Gulf of Trieste. *International Regional Conference Pollution of the Mediterranean Sea, Split: 337-349.*
- O R L I ć, M. 1988. Report of Yugoslav-Italian Commission for the protection of the Adriatic Sea, pp. 233-244.
- O r l i ć, M. 1989. Salinity of the North Adriatic: a fresh look at some old data. *Boll. Oceanogr. Teor. Appl.*, 3: 219-228.
- R a j a r, R. and M. Č e t i n a. 1986. Mathematical simulation of two-dimensional lake circulation. In M. Radoković, Č. Maksimović, C.A. Brebbia (Eds.), *HYDROSOFT Conference* Southampton, Springer Verlag, pp. 125-134.
- R a j a r, R. 1989a. Three dimensional modelling of currents in the Northern Adriatic sea. *XXIII Congress IAHR, Ottawa: 335-342.*
- R a j a r, R., M. Č e t i n a, V. T o n i n. 1989b. Influence of licarization and of vertical distribution of turbulent viscosity coefficient on three-dimensional simulation of currents. In: Č. Maksimović, M. Radojković (Eds.), *HYDROCOMP 89, International Conference of Interaction of Computational Measurements in Hydraulics and Hydrology, Dubrovnik, June 13 - 16, pp. 193-202.*
- R a j a r, R. 1990. Three dimensional mathematical model of currents and of transport of pollutants in the Adriatic. In: G. Gambolati *et al.* (Ed.), *International Conf. on Computational Methods in Water Resources, Venice, June, pp. 57-62.*
- R a j a r, R. 1992. Mathematical modelling of currents and of dispersion in Slovenian coastal water. Report, University of Ljubljana, 1992.
- R o d i, W. 1980. Turbulence models and their applications in hydraulics. *IAHR Publications, Delft, 104 pp.*
- S t r a v i s i, F. 1977. Bora driven circulation in the Northern Adriatic. *Boll. Geofis. Teor. Appl.*, 19: 95-102.
- T o n i n, V. 1986. Study of hydrodynamic conditions of coastal sea. Report. Water Management Institute, Ljubljana.
- T u r k, V., J. F a g a n e l i and A. M a l e j. 1982. A look at the pollution problems in the Bay of Koper (North Adriatic) in relation to the provisional sewage outfall. *Rep. Comm. int. Mer Mediterr.*, 603-608

MODELIRANJE STRUJANJA IZAZVANOG MORSKIM MIJENAMA I
VJETROM I DISPERZIJE U
SJEVERNOM JADRANU

R. R a j a r i M. Č e t i n a

*Sveučilište u Ljubljani, Fakultet gradjevinarstva i istraživanja u
gradjevinarstvu, Ljubljana Slovenija*

KRATKI SADRŽAJ

U prvom redu opisan je nelinearni trodimenzionalni baroklini model razvijen pri Odjelu za inženjering u gradjevinarstvu na Sveučilištu u Ljubljani. Vertikalna turbulentna viskoznost u modelu računata je iz jednadžbe turbulentnog modela K o u t i t a s a, dok je horizontalno uzeta homogena viskoznost.

Modelom je računato plimno strujanje u Tršćanskom zaljevu. M2 komponenta morskih mijena uzeta je za rubni uvjet na otvorenim granicama. U cilju određivanja plimnog strujanja u manjem Piranskom i Koparskom zaljevu rezultati simuliranja u širem akvatoriju uzeti su za rubne uvjete. Mjerenja struja duž slovenske obale koja su izvršili članovi Menagementa za vodu Instituta u Ljubljani u periodu od 1984. do 1986. uzeta su za verifikaciju modela. Podudarnost rezultata je relativno dobra. Mjerenja kao i simulacija ukazuju na ciklonski vrtlog u Koparskom zaljevu tijekom oseke i rezidualno strujanje veličine 3 do 6 cm/s izmjereno u Koparskom zaljevu smjera je od istočnog do sjevernog. Mjerenja takodjer ukazuju na slabije rezidualno strujanje od istočnog do sjeveroistočnog smjera duž cijele slovenske obale prema Trstu intenziteta 1 do 3 cm/s.

Disperzija zagadivača iz rijeke Rižane u Koparski zaljev simulirana je i kvalitativno uspoređena sa disperzijom fekalnih zagadivača.

S istim trodimenzionalnim modelom simulirano je strujanje prouzročeno vjetrom kao i transport i disperzija vode rijeke Pad u sjevernom Jadrano. Strujanje prouzročeno burom dobro se slaže sa satelitskim mjerenjima koncentracije klorofila (prema K u z m i ć u). Strujanja prouzročena burom i jugom simulirana su za zimsku situaciju bez stratifikacije kao i za ljetnu sa stratifikacijom. U oba slučaja, i za bure i za juga, simulacija pokazuje da se dio zagadjene vode rijeke Pad transportira prema obalama Slovenije i Hrvatske.